NMR study of ordering kinetics in Ni_3Al alloys

Patrick Scherrer and Costas Dimitropoulos
Institut de Physique Expérimentale, Ecole Polytechnique Fédérale de Lausanne, CH-1015 Lausanne, Switzerland

Ferdinando Borsa
Dipartimento di Fisica ''A. Volta'' and INFM, Università di Pavia, I-27100 Pavia, Italy
and Ames Laboratory and Department of Physics, Iowa State University, Ames, Iowa 50011

Silvia Rubini*
Dipartimento di Fisica ''A. Volta,'' Università di Pavia, I-27100 Pavia, Italy
(Received 11 August 1997; revised manuscript received 22 December 1997)

^{27}Al nuclear magnetic resonance (NMR) and relaxation has been applied to the study of the effects of ball milling on the long-range order (LRO) of fcc $L1_2$ Ni_3Al as well as to the subsequent microscopic reordering process through annealing. Structural changes due to the mechanical treatment are correlated to the appearance of a strong magnetization in the disordered phase. In the absence of significant Fe contamination, this magnetic property is attributed to the existence of magnetic moments of the order of $0.23\,\mu_B$ (μ_B=Bohr magneton) localized at the Ni sites. ^{27}Al NMR spectra in both the ordered and the disordered phase are presented. The random distribution of atoms combined with the magnetic properties in the disordered phase cause a substantial broadening of the ^{27}Al NMR line. The linewidth is proportional to the fractional change of disorder and is therefore used to monitor the ordering transformation as a function of annealing time and temperature. The changes of spin-lattice relaxation rates (T_1^{-1}) and Knight shifts during transformation are also examined. The overall ordering behavior as observed by NMR is described in terms of a stretched exponential for the time dependence of the untransformed fraction, implying a time-dependent transformation rate. The activation energy of the Ni vacancy migration mechanism responsible for the transformation was determined to be $E=1.8\ \mathrm{eV}\pm0.2\ \mathrm{eV}$. The average distance covered by the atoms during the ordering is estimated by means of a simple random-walk model. [S0163-1829(98)09317-5]

I. INTRODUCTION

The ordered Ni_3Al intermetallic alloy exhibits excellent high-temperature strength and corrosion resistance. Brittleness and poor ductility at room temperature, however, seriously hinder easy shaping of the alloy. Nevertheless, formability can be improved by the introduction of a disordered metastable state more suitable for machining processes. The initial ordered state and its interesting high-temperature properties are subsequently recovered by annealing the alloy.

The understanding of ordering mechanism in metallic systems has still many aspects to be clarified. The problem addressed here is the long-range ordering (LRO) process[1] in a metallic alloy initially prepared in a metastable disordered state. With the term LRO, we indicate a crystalline arrangement in which atomic species reside on distinct sublattices as opposed to a random distribution over lattice sites.

The intermetallic compound Ni_3Al crystallizes in an ordered face-centered-cubic structure ($L1_2$) with Ni atoms at the face centers and Al atoms at the cubic corners. Among the methods to introduce disorder, one of the most effective is mechanical milling.[2,3] Once the metastable disordered state is obtained, the kinetics of its reordering can be studied by various techniques including x-rays, positron annihilation, calorimetry, electric resistivity, magnetization, etc.[4–7] In the present study, we introduce NMR as a technique to investigate the ordering of the metastable disordered fcc state in Ni_3Al. The ^{27}Al nucleus is a microscopic probe of the local atomic arrangement and of the local magnetic properties of the transition (Ni) atoms. Magnetic properties related to the degree of order in intermetallic Ni_xAl_{1-x} have been reported.[8,9] As will appear from magnetization measurements, the disordering of the Ni_3Al alloy introduces a ferromagnetic moment at the Ni site with $\mu_{\mathrm{eff}}=0.2-0.3\mu_B$. Thus the combination of the Ni magnetic moment and the random distribution of Ni atoms in the disordered phase induces a severe broadening of the ^{27}Al NMR line via the hyperfine coupling of the Ni atomic moments to the ^{27}Al nuclei. Therefore, it is justified to introduce the ^{27}Al NMR linewidth as a parameter related to the degree of LRO and to use its temperature and time dependence to investigate the kinetics of ordering.

In Sec. II we discuss the preparation of the samples and the experimental methods. In Sec. III we present the experimental data with particular emphasis on the linewidth data as a function of annealing time for different annealing temperatures. The data are parametrized with a time dependence of the untransformed disordered phase described by a stretched-exponential function. Comparison of NMR and x-ray-diffraction measurements are presented in Sec. IV. Qualitative agreement between the different methods is shown to be satisfactory. In Sec. V we discuss the physical significance of the experimental observations in terms of simple models describing the reordering as the result of random-walk diffusion of Ni and Al atoms. The summary and conclusions are given in Sec. VI.

II. EXPERIMENTAL DETAILS

A. Sample preparation

An ingot of the ordered Ni_3Al alloy was prepared by melting the proper amounts of high-purity metals (99.999 wt. %). Homogenization of the alloy was obtained by annealing the ingot at 1473 K during 7 days in a sealed Ta tube under Ar atmosphere. Part of the ingot was filed with a corundum grindstone and the powdered alloy was then subjected to ball milling for 8 h. To avoid thermal activation and eventual partial reordering, the powder was intermittently cooled with liquid nitrogen to 78 K during the mechanical treatment. Contamination with ferromagnetic impurities (Fe) was investigated by electron microprobe analysis on a Leica 430 scanning electron microscope equipped with an Oxford ISIS x-ray spectrometer. No trace of Fe contamination was detected implying an iron concentration $<0.1\%$. The disordered powder (average grain size of 1–50 μm) was divided into several identical small samples (300 mg each). Each sample was utilized to investigate the ordering kinetics at a different annealing temperature.

B. Calorimetry, x rays, and magnetic measurements

The metastability of the disordered state in the ball-milled Ni_3Al was tested by differential scanning calorimetry (DSC). The sample was heated to 800 K in a computer-assisted calorimeter (Mettler TA4000) at a heating rate of 10°/min.

X-ray-diffraction (XRD) measurements were used to characterize the structural changes resulting from ball milling. The XRD patterns have been recorded on a powder diffractometer (Rigaku BD MAX) using monochromated Cu $K\alpha$ radiation. The powder was spread out on an adhesive glass plate which was then mounted on a high-precision goniometer.

The magnetic properties of the sample have been evaluated by magnetization measurements on a superconducting quantum interference device susceptometer (Quantum Design MPMS-7) with applied external fields up to 1.5 T at room temperature.

C. NMR measurements

Standard pulse NMR techniques have been applied for ^{27}Al absorption spectra and relaxation time measurements. The experimental setup consisted of an Oxford 8 T NMR Magnet with a 50 mm diameter variable-temperature (4–400 K) bore, an Amplifier Research AR200L rf-pulse power amplifier (output level of 400 W) and a Bruker Z20A signal preamplifier completed by a homebuilt low-dead-time spectrometer. For selected field-dependent measurements, an Oxford 14 T NMR magnet as well as a Varian 2 T electromagnet were also available. Typical pulse widths obtained with homebuilt NMR probes were around 5 μs. For the spin-echo measurements the time interval between the two pulses and the repetition rate have been set, respectively, to 30 μs and 150 ms. Due to incomplete irradiation of the broad ^{27}Al line in the disordered samples, a point by point spin-echo reconstruction technique had to be applied for spectrum acquisition. Each point on the spectrum represents the measured echo amplitude for the corresponding irradiation frequency. From the Larmor frequency ν_L, the exact value of the Knight shift,[10] $\mathcal{K}=(\nu_L-\nu_{\mathrm{ref}})/\nu_{\mathrm{ref}}$, was calculated with respect to the ^{27}Al resonance frequency ν_{ref} in $AlCl_3$ aqueous solution. Except for the measurements of ^{27}Al linewidth vs temperature, all other measurements were performed at equilibrium at room temperature after a given annealing procedure characterized by an annealing time t_A and an annealing temperature T_A.

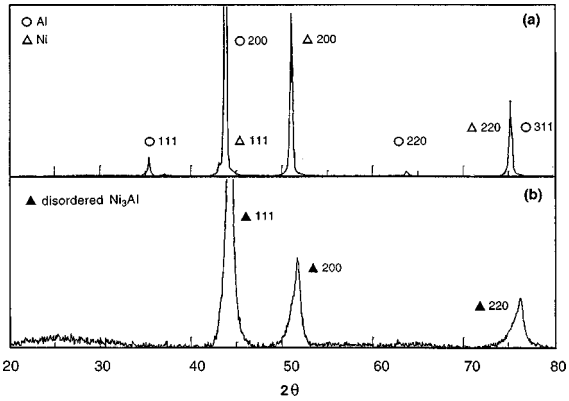

FIG. 1. X-ray-diffraction patterns of Ni_3Al samples (a) before ball milling (ordered) and (b) after 8 h of ball milling (disordered).

III. RESULTS

A. Calorimetry, x rays, and magnetization

DSC curves show a broad predominant exothermic peak at 683 K attributed to the ordering of the alloy[11] from fcc Ni_3Al to $L1_2$ Ni_3Al. A smaller exothermic contribution which is detected around 500 K is due to the formation of fcc Ni_3Al.

Both the ordered and disordered Ni_3Al were characterized by powder x-ray diffraction as shown in Fig. 1. The diffraction pattern of the ordered alloy exhibits the sharp typical lines for $L1_2$ ordered fcc structure.[11,12] The ball-milled alloy is found to be strongly disordered after 8 h of mechanical treatment. The intensity of the fundamental (111), (200), and (220) lines are significantly reduced while a severe broadening with a marked asymmetry on the low angle side is detected.

The magnetization curves as function of the applied field at room temperature in the ordered and the disordered phase exhibit a weak hysteresis (Fig. 2). The magnetization at saturation (M_S) is reached for magnetic fields >0.5 T and NMR measurements (2 to 14 T) are therefore performed under saturation conditions. The value of M_S turns out to be 100 times higher in the disordered phase than in the ordered one. Once more, the presence of substantial ferromagnetic impurities (Fe) can be ruled out. The observed behavior is indeed contrary to what would be expected in case of Fe contamination. It has been shown that the magnetization in Fe-doped disordered Ni_3Al is significantly lower than in the ordered phase due to a smaller number of Ni-Fe magnetic nearest neighbors.[13] From the value of M_S, the magnitude of the magnetic moment μ_{eff} attributed to a Ni site is estimated in terms of Bohr magnetons by means of the following relation:

$$\mu_{\mathrm{eff}}=\frac{1}{3}\frac{M_s m_{\mathrm{Ni_3Al}}}{N_{\mathrm{Av}}\mu_B}, \tag{1}$$

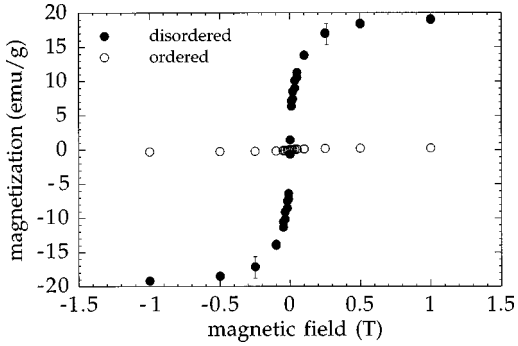

FIG. 2. Magnetization as a function of the applied magnetic field in ordered and disordered Ni_3Al, respectively. In both cases, a weak hysteresis is detected. The saturation magnetization M_S is 100 times higher in the disordered state.

where M_S is the saturation magnetization per unit mass, N_{Av} is the Avogadro number, and $m_{\mathrm{Ni_3Al}}$ is the molar mass of the Ni_3Al alloy. From the experimental results we get $\mu_{\mathrm{eff}} = 0.23\mu_B/\mathrm{Ni\ atom}$.

B. ^{27}Al NMR spectra

The ^{27}Al NMR spectrum is shown in Fig. 3 for both the alloy with the degree of disorder obtained from ball milling and the fully ordered alloy. The narrow line of the ordered alloy is asymmetric as shown in Fig. 4, with the asymmetry depending linearly on the magnetic field. The line shape can be fitted with a powder pattern typical of axially symmetric anisotropic Knight shift convoluted with a Lorentzian broadening.[14,15] An anisotropic Knight shift $\mathcal{K}_{\mathrm{ax}} = 1/3[(\upsilon_{\parallel} - \upsilon_{\perp})/\upsilon_{\mathrm{ref}}] = -0.05 \pm 0.01\%$ at the ^{27}Al site, however, would imply an axial point symmetry such as would result from a tetragonal distortion of the fcc lattice for which there is no evidence in the x-ray pattern. More likely the asymmetric line results from the presence of several Al sites for which the resonance frequency is shifted by the presence of clusters of Ni atoms which bear a residual local paramagnetic moment. The ^{27}Al line broadening due to the homonuclear dipolar interaction and estimated from the Van Vleck second moment[16,17] is 2.4 kHz. The ^{27}Al NMR linewidth in the disordered alloy is only weakly field dependent in the range of 2 to 14 T. This is consistent with the notion that the inhomogeneous broadening in the disordered alloy is associated with the presence of ferromagnetically aligned magnetic

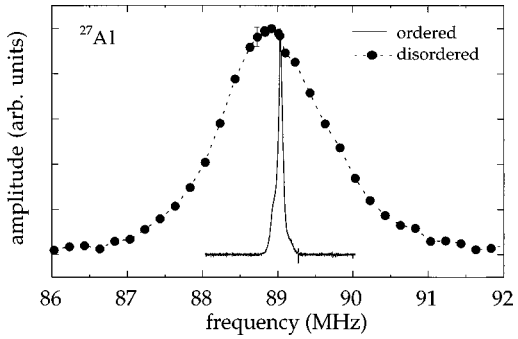

FIG. 3. ^{27}Al spectra in ordered and disordered Ni_3Al, respectively, for an external field of 8 T. The line in the disordered state is reconstructed point by point as discussed in the text.

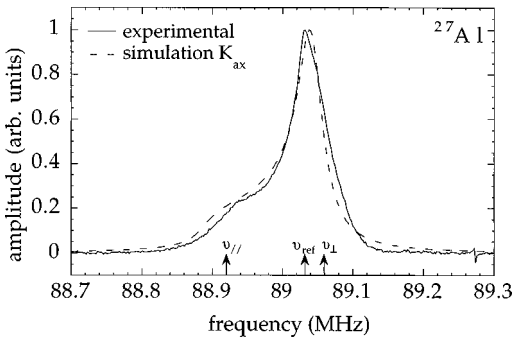

FIG. 4. ^{27}Al spectrum in ordered Ni_3Al for an external field of 8 T. The dotted line represents the theoretical powder spectrum resulting from an anisotropic axially symmetric Knight shift with a Lorentzian broadening of 40 kHz.

moments at the Ni sites. The local environment of Al nuclei is different from site to site as a consequence of the random occupation of lattice sites by Ni and Al. As a consequence, the Al nucleus experiences a distribution of local fields proportional to the Ni magnetization whereby the magnetization is almost saturated above 2 T as shown in Fig. 2.

The ^{27}Al linewidth in the disordered alloy is plotted as a function of temperature in Fig. 5. These linewidths are subject to a combination of motional narrowing due to the diffusion of Ni and Al atoms on the lattice and a static narrowing due to the reordering. The observed effect in Fig. 5 can be described by the Kubo-Tomita formula[17]

$$\Delta\upsilon^2 = \langle \Delta\upsilon_0^2 \rangle \frac{2}{\pi} \arctan(\delta\upsilon \cdot \tau), \tag{2}$$

where $\Delta\upsilon^2$ is the second moment of the NMR line and $\delta\upsilon \approx \sqrt{\Delta\upsilon^2}$ is the half linewidth. $\langle \Delta\upsilon_0^2 \rangle$ is the rigid lattice second moment.

Ideally, the experimental procedure for such a measurement would consist of a heating at a constant rate with very short measurement times at selected temperatures. The time necessary for the acquisition of a single NMR spectrum is however of the order of 300 s. Thus, the experimental procedure should rather be considered as a stepwise annealing in which the sample heating is interrupted to maintain the tem-

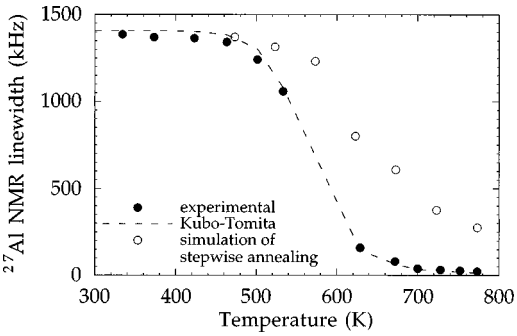

FIG. 5. Full width at half magnitude of the ^{27}Al line as a function of temperature for an external field of 2 T (black dots). The dashed line corresponds to the best fit according to the Kubo-Tomita formula. The circles represent the linewidths one would measure at room temperature for a stepwise annealing as discussed in the text.

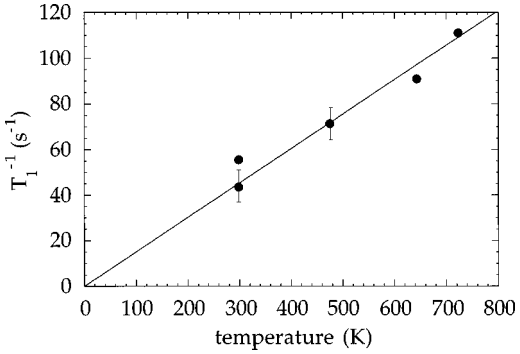

FIG. 6. ^{27}Al spin-lattice relaxation rate T_1^{-1} in ordered Ni_3Al as a function of temperature. The full line is a best fit according to the Korringa law $(T_1T)^{-1}=0.143\ s^{-1}\ K^{-1}$.

perature stable for the time of the NMR measurement. Basing on this fact and on results of isothermal annealing, we will discuss in Sec. V how the observed linewidth behavior can be roughly foreseen and reproduced as illustrated in Fig. 5.

C. ^{27}Al Knight shift and nuclear spin-lattice relaxation rate

The values of the ^{27}Al nuclear spin-lattice relaxation rate have been determined from a single exponential decay behavior of the magnetization. One might expect the magnetization to decay nonexponentially due to diffusional processes. In our case, however, a single exponential decay is observed. Such a simple behavior is coherent with the fact that the T_1^{-1} measurements have been performed at room temperature after the annealing procedure under conditions where the thermally activated diffusion process leading to the ordering of the material is negligible.

The ^{27}Al nuclear spin-lattice relaxation rate is shown in Fig. 6 as a function of temperature in the ordered alloy. The relaxation rate was found to be independent from the applied magnetic field. The linear temperature dependence with $(T_1T)^{-1}=0.143\ s^{-1}\ K^{-1}$ and the lack of frequency dependence indicate a relaxation mechanism dominated by the interaction of Al nuclei with the conduction electrons (Korringa law[17]) with no measurable contribution from atomic motion. The value of $(T_1T)^{-1}=0.143\ s^{-1}\ K^{-1}$ in Ni_3Al is intermediate between the one in pure Al metal: $(T_1T)^{-1}=0.54\ s^{-1}\ K^{-1}$ (see Ref. 10) and the one in NiAl near the equiatomic composition: $(T_1T)^{-1}=0.03\ s^{-1}\ K^{-1}$ (see Ref. 18). So far, no ^{27}Al T_1 values have been reported in the literature for Ni_3Al. However, the value of 23 ms obtained at room temperature in the ordered alloy is consistent with spin-lattice relaxation times measured in Ni-rich β-NiAl and extrapolated to a concentration of 75 at. % Ni.[19] The Knight shift estimated from the Korringa ratio $(T_1T\mathcal{K}^2)^{-1}=4\pi k_B/\hbar(\gamma_N/\gamma_e)^2$ is of the order of 0.08%, while the isotropic part of the shift estimated experimentally is about $\mathcal{K}_{iso}=-0.02\pm0.01\%$. The fact that the two values are completely different indicates that the measured shift is dominated by a mechanism different from the coupling to the conduction electrons, which determines the Korringa ratio, as discussed further on. The evolution of the spin-lattice relaxation rate and of the Knight shift measured at room temperature at the center of gravity of the broad NMR spectrum

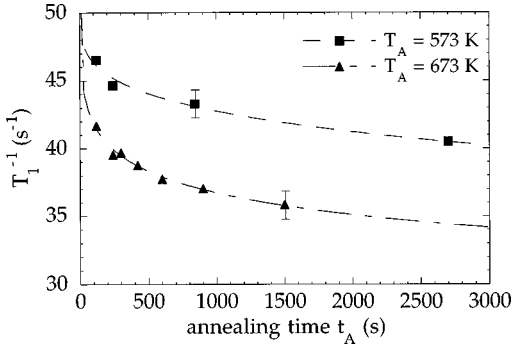

FIG. 7. ^{27}Al spin-lattice relaxation rate measured at room temperature in the disordered alloy as a function of annealing time for two different annealing temperatures T_A. The dotted lines are guides for the eye.

in the disordered alloy as a function of annealing time are shown in Figs. 7 and 8, respectively.

Since the ^{27}Al NMR lines in the disordered phase are very broad, both the T_1^{-1} and the Knight-shift data in Figs. 7 and 8 have to be viewed only as indicative. The large negative shifts observed in the disordered phase are most likely due to the average hyperfine field generated at the Al site by the ferromagnetic Ni moments and are thus not Knight shifts related to the electronic band structure. This is confirmed by the lack of correlation between the large changes in $\mathcal{K}$ in Fig. 8 and the relatively small changes of T_1^{-1} in Fig. 7.

D. ^{27}Al NMR linewidth vs annealing time and vs annealing temperature

The full ^{27}Al NMR linewidth in the completely disordered phase is about 1400 kHz. The inhomogeneous broadening is due to the distribution of local hyperfine fields arising from the random arrangement of Ni magnetic moments around a given Al nucleus as discussed in Sec. III B. In Fig. 9, the ^{27}Al NMR spectra measured on a disordered sample following different annealing times at temperature $T_A=773$ K are shown. As the system becomes more ordered, the linewidth decreases until it reaches a value close to the one in the ordered alloy. The recovery, however, is never complete, even for very long annealing times. In order to

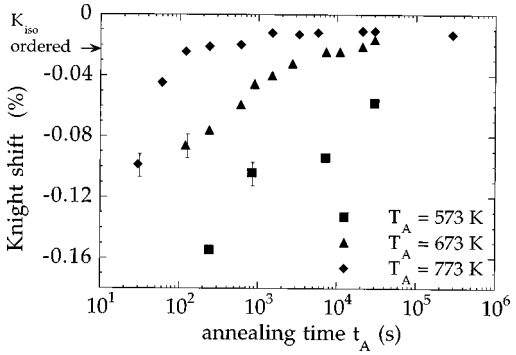

FIG. 8. ^{27}Al Knight shift measured at room temperature in the disordered alloy as a function of the annealing time for three different annealing temperatures T_A. As the system reorders, the value of the Knight shift tends towards the isotropic shift of the ordered system indicated by the arrow.

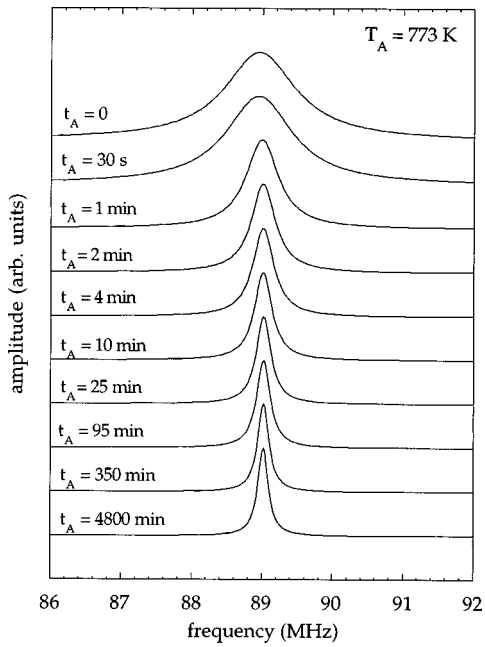

FIG. 9. ^{27}Al spectra measured at room temperature as a function of annealing time at $T_A = 773$ K for a magnetic field of 8 T. The linewidth (initially 1400 kHz) narrows towards the width of the ordered state.

describe quantitatively the ordering kinetics, we assume that the contribution of the random electronic Ni magnetic moments to the total second moment can be added to the background second moment of the ordered phase:

$$\langle \Delta \nu^2 \rangle_{\text{measured}} = \Omega^2 \langle \Delta \nu^2 \rangle_{\text{disordered}} + (1-\Omega^2) \langle \Delta \nu^2 \rangle_{\text{ordered}}. \tag{3}$$

Following Eq. (3), we estimate the fraction of disordered alloy from the analysis of the measured linewidth and we calculate Ω as

$$\Omega(t_A, T_A) = \sqrt{\frac{\langle \Delta \nu^2(t_A, T_A) \rangle_{\text{measured}} - \langle \Delta \nu^2 \rangle_{\text{ordered}}}{\langle \Delta \nu^2 \rangle_{\text{disordered}} - \langle \Delta \nu^2 \rangle_{\text{ordered}}}}. \tag{4}$$

Thus we plot in Fig. 10 the untransformed fraction Ω obtained by subtracting from the square of the measured width the square of the linewidth of the ordered phase (full linewidth=180 kHz) and normalizing it with respect to the linewidth of the disordered state. One could decide to plot directly the measured linewidth or to use a different procedure to extract the contribution related to the disorder without changing the main qualitative conclusions reached in the following.

The linewidths yielding $\Omega(t_A, T_A)$ in Fig. 10 were measured at room temperature after having annealed the sample at a given temperature T_A for a given time t_A. Each curve corresponds to a different annealing temperature T_A and for each one we start with a virgin sample initially in the disordered phase. The increase of annealing time t_A for each curve was obtained by using the same sample. In each step, the sample was annealed for a time t'_A, cooled down to room temperature where the linewidth was measured, then heated back to the same annealing temperature T_A, left there for a time t''_A, cooled to room temperature and so on. The total

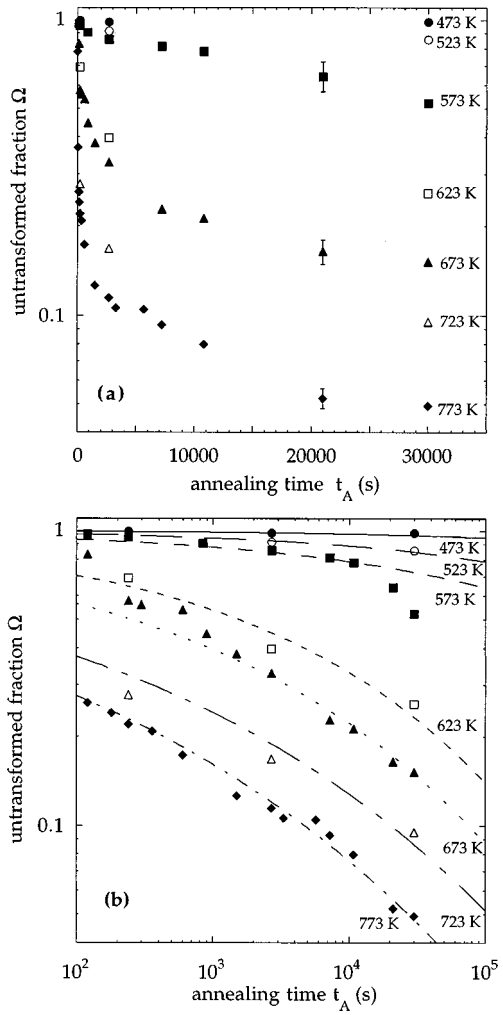

FIG. 10. Isothermal annealing curves of Ni_3Al as obtained from the ^{27}Al NMR linewidth. (a) On the lin-log scale, the asymptotic behavior of the ordering process is emphasized. The fully ordered phase is never completely reached. (b) On the log-log scale, the initial fast decrease of the linewidth is shown more explicitly.

annealing time in Fig. 10 is then given by $t_A = t'_A + t''_A + t'''_A + \cdots$ and the lin-log plot shows a rapid initial decrease of the linewidth followed by a tail at long time. The time dependence can be parametrized by fitting the curves with a stretched-exponential function:

$$\Omega(t_A, T_A) = \exp -(A(T_A) t_A)^{\beta(T_A)}. \tag{5}$$

The result of the fit is shown in Fig. 10(b) where now a log-log plot is chosen to emphasize the importance of the initial fast decrease of the linewidth. The parameters obtained from the fits are shown in Table I. The parameter $A(T_A)$ which represents an effective transformation rate for the kinetics of reordering of the alloy is shown in Fig. 11 plotted as a function of the inverse annealing temperature $1/T_A$.

IV. COMPARISON BETWEEN NMR AND X-RAY RESULTS

The ordering process of Ni_3Al has been studied by means of several standard experimental techniques. In particular,

TABLE I. Transformation rate $A(T_A)$ of the ordering process and exponent β of the stretched exponential as obtained by fitting the experimental data to Eq. (5).

Annealing temperature T_A (K)	$A(T_A)$ (s^{-1})	$\beta(T_A)$
473	1.0×10^{-9}	0.32
523	1.0×10^{-7}	0.31
573	5.0×10^{-7}	0.27
623	1.5×10^{-4}	0.25
673	7.0×10^{-4}	0.21
723	9.0×10^{-3}	0.16
773	5.5×10^{-2}	0.15

x-ray diffraction offers a suitable way of validation for the NMR results presented here. For XRD, the fractional change Ω_{RX} has been defined on the basis of the integrated intensities of selected lines as

$$\Omega_{RX}=\frac{[S_{111}(t_A)/S_{200}(t_A)]-(S_{111}/S_{200})_{\text{Ordered}}}{[S_{111}(0)/S_{200}(0)]-(S_{111}/S_{200})_{\text{Ordered}}}, \qquad (6)$$

where S is the area of the line identified by the corresponding index in Fig. 1(b). The untransformed fraction of disordered phase as function of annealing time for the NMR and the x-ray method are compared in Fig. 12 for $T_A=773$ K. The agreement is satisfactory.

V. DISCUSSION

As seen in Fig. 11, the effective transformation rate $A(T_A)$ which determines the kinetics of ordering can be described by an activated law $A(T_A)=A_0\exp-(E_A/k_BT_A)$ with $A_0=5\times10^{-10}$ s^{-1} and $E_A/k_B=21\,100\pm2000$ K (i.e., $E_A=1.8\pm0.2$ eV). The activation energy measured here fits remarkably well into a series of earlier published values for Ni_3Al [$E_A=1.65$ eV,[4] $E_A=1.78$ eV (Ref. 12)], especially considering that the results have been obtained with different experimental techniques and data analysis methods. In general, it is a well accepted concept that the ordering process in Ni_3Al is driven by a Ni vacancy diffusion mechanism (see, for instance, Refs. 4 and 12). These vacancies are introduced by the mechanical treatment applied to the alloy during ball milling. Thus, the thermally activated ordering process of the material does not involve formation of vacancies as these are already present at very high concentration. The process is then essentially one of vacancy diffusion characterized by the migration energy E_V^M. As a consequence, the activation energy E_A of the ordering may be mainly assigned to the movement of the vacancies and hence represent a reasonable estimate of E_V^M. It has already been shown that such an assumption is reasonable for Ni vacancy diffusion in cold-rolled nickel.[20] With regards to the mechanical treatment, it should be noticed that heavily strained samples can exhibit an ordering process with energetical parameters different from those of relaxed samples.[12] Such discrepancies in the energetical parameters are also found between irradiated Ni (Ref. 21) and cold-rolled Ni.[20]

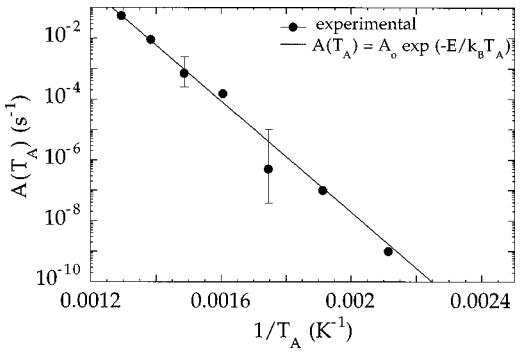

FIG. 11. Transformation rate of the ordering process in Ni_3Al as function of the inverse annealing temperature. On the lin-log scale the exponential dependence appears as a straight line.

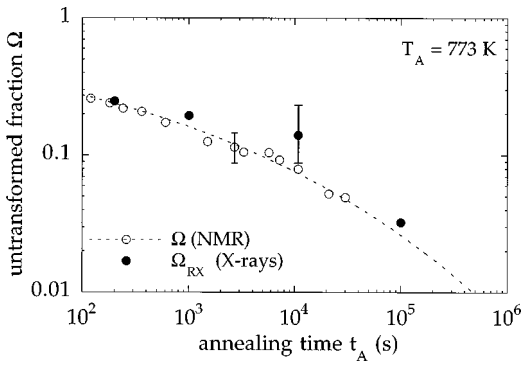

FIG. 12. Untransformed fraction of disordered phase measured at room temperature as function of annealing time for an annealing temperature $T_A=773$ K for both NMR and x rays.

At this point, one could argue that the activation energy might be extracted as well from the line narrowing measurements presented in Fig. 5. By assuming for the correlation time τ an activated temperature dependence $\tau=\tau_0\exp(E/k_BT)$, the experimental data in Fig. 5 can indeed be fitted by Eq. (2) with $\tau_0=10^{-13}$ s and $E/k_B=8715\pm200$ K. This value is quite different from that extracted from the isothermal curves (i.e., 21 100 K) as one expects, since the short-range atomic motions which determine the NMR line narrowing process can be different from the long-range ones responsible for the ordering process. In order to compare the two processes, we start by noting that, due to the rather long times needed for the linewidth measurements, the heating procedure performed to collect the experimental data in Fig. 5 is quite similar to a stepwise annealing. The observed linewidth reported in Fig. 5 is therefore the result of two different contributions: the narrowing resulting from the irreversible change of the atomic arrangement and of the Ni local moments due to the ordering process that takes place during the duration of the experiment, and the motional narrowing due to the self-diffusion of Al atoms occurring at the temperature at which measurements are performed. One can tentatively separate the contribution of the two mechanisms by calculating from the isothermal curves of Fig. 10(b) the linewidth that one would measure at room temperature after each step of a stepwise annealing process that simulates the series of measurements of Fig. 5. In other words, one could think that for each thermal step, the evolution of the linewidth follows the corresponding isothermal curve. Heating the sample to the next higher temperature is equivalent to a jump between the corresponding isothermal curves. The

results of this simulation are also reported in Fig. 5. They have been validated by the experimental measurement of a 400 kHz linewidth after a stepwise annealing up to 723 K, in very good agreement with the simulation results. The overall temperature dependence of the experimental NMR linewidth data is similar to the behavior of the linewidth obtained from the simulation of stepwise annealing whereby the difference between the two sets of data should be ascribed to the motional narrowing effects due specifically to the equilibrium random thermal motion of the atoms. We conclude that a reordering process controlled by the high activation energy derived from the isothermal annealing curves is consistent with the linewidth behavior in Fig. 5.

What remains to be explained is the fact that the apparent activation energy derived from ^{27}Al NMR line narrowing is more than a factor of 2 smaller than the one derived for the ordering process. The discrepancy is most likely due to the fact that the NMR linewidth at any given temperature is narrowed mostly by the Al local atomic motion. This explanation is consistent with the data of migration enthalpies in fcc metals[21] which yield for Al a value almost a factor of 2 lower than for Ni.

Let us now come back to the isothermal linewidth behavior. The stretched-exponential law [Eq. (5)] can be justified as follows: when the system is first heated to the annealing temperature T_A, the ordering occurs via diffusion in presence of a large relative concentration of vacancies C_V^0 present in the disordered alloy due to the ball-milling treatment. This concentration is much higher than the equilibrium thermal concentration of vacancies. As the ordering proceeds in time, the initial concentration of vacancies C_V^0 decreases and correspondingly the thermal hopping frequency of the atoms diminishes. This slowing down of the diffusion generates the characteristic stretched-exponential behavior as already observed in similar processes where the effective diffusion coefficient decreases as a function of time.[22] The proposed stretched-exponential formula describing the ordering process as observed by NMR [Eq. (5)] can indeed be rewritten as a simple exponential

$$\Omega(t_A,T_A)=\exp-(A'(t_A,T_A)t_A), \tag{7}$$

provided that one introduces a time-dependent transformation rate

$$A'(t_A,T_A)=A(T_A)^{\beta(T_A)}t_A^{\beta(T_A)-1}. \tag{8}$$

Equations (5) and (7) illustrate that different expressions can fit the data as may be expected from a complex diffusion process with several parameters depending on temperature and time. Equation (7), however, is most relevant to the physical aspect of the process, as it shows that the real physical effect rests in the time dependence of the transformation rate. We justify now the time-dependent transformation rate [Eq. (8)] in terms of a simple random-walk diffusion process[23] through vacancies. Let us define ν_V as the attempt frequency of a vacancy and ν_A as the attempt frequency of an atom (Al or Ni). From the detailed balance one has

$$\nu_V C_V=\nu_A C_A, \tag{9}$$

where C_V and C_A are the concentrations of vacancies and atoms, respectively. The attempt frequency of a vacancy is written as $\nu_V=\nu_V^0\exp-(E_V^M/k_BT)$. The prefactor ν_V^0 can be estimated as the vibrational frequency of an atom in its potential well. From a simple harmonic oscillator model, one has

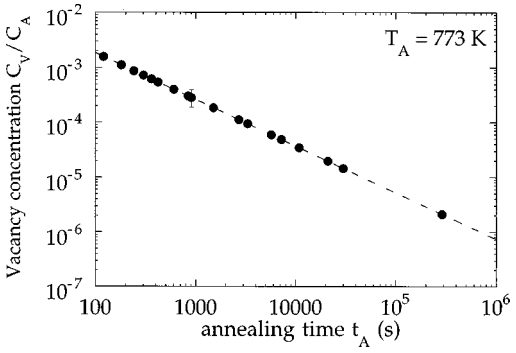

FIG. 13. Relative vacancy concentration in the disordered alloy as function of annealing time for $T_A=773$ K. The dotted line corresponds to Eq. (12) with $\beta=0.15$.

$$\nu_V^0=\frac{1}{d\sqrt{2}}\sqrt{\frac{E_b}{m}}, \tag{10}$$

where m is the mass of the ion, d is the distance from the ion to the vacant site, and E_b is the height of the potential barrier. For $E_b/k_B=E_A/k_B=21\,100$ K, $m=61$ a.u. (Ni atom), and $d=a/\sqrt{2}=2.52$ Å (distance between Ni and Al sites), one has $\nu_V^0=5\times10^{12}$ s^{-1}. Despite the model's simplicity, a vibrational frequency of the order of 5 THz for the Ni atoms is very reasonable. This is confirmed by recently published vibrational density of states (DOS) calculations in ordered and disordered Ni_3Al.[24] If we identify $A'(t_A,T_A)$ in Eq. (8) as the atomic attempt frequency ν_A then

$$A'(t_A,T_A)=\frac{C_V(t_A,T_A)}{C_A}\,\nu_V^0\exp-\left(\frac{E_V^M}{k_BT_A}\right), \tag{11}$$

where the activation energy E_A has been identified to the Ni vacancy migration energy E_V^M. Thus, the time dependence of the transformation rate follows from the time dependence of the vacancy concentration. The relative vacancy concentration $C_V(t_A,T_A)/C_A$ is obtained from Eqs. (8) and (11) as

$$\frac{C_V(t_A,T_A)}{C_A}=\frac{A(T_A)^{\beta(T_A)}t_A^{\beta(T_A)-1}}{\nu_V^0}\exp\left(\frac{E_V^M}{k_BT_A}\right). \tag{12}$$

C_V/C_A is plotted as a function of annealing time in Fig. 13 showing a power-law decay in annealing time with an exponent $\beta-1=-0.85$ (see Table I for $T_A=773$ K). The values obtained for short annealing times correspond to very high concentrations of intrinsic vacancies as postulated initially.

In a simple random-walk model, the mean-square displacement of the diffusing atom is $\langle r^2\rangle=Nd^2$ where N is the number of jumps and d is the jump distance. The diffusion coefficient being defined as $D=(1/6)d^2\nu_A$, where ν_A is the effective hopping frequency of the atoms, the time to cover the distance is given by $t=(1/6D)\langle r^2\rangle=(1/6D)Nd^2=N\nu_A$. Once again, if we identify $\nu_A=A'(t_A,T_A)$, we can write for a small time interval

$$\frac{dN}{dt} = A'(t, T_A). \tag{13}$$

Therefore $N = \int_0^{t_{AF}} A'(t, T_A) dt$, where t_{AF} is the time necessary to complete the ordering. Using Eq. (8) we finally find

$$N = A(T_A)^{\beta(T_A)} \frac{t_{AF}^{\beta(T_A)}}{\beta(T_A)}. \tag{14}$$

With the experimental values found for $A(T_A)$ and t_{AF}, Eq. (14) yields

$$16 \leqslant N \leqslant 36. \tag{15}$$

These values show that the mean distance covered by the particles during the ordering process is of a few lattice parameters only (4–6), which is coherent with the high vacancy concentration in the disordered alloy. From a quantitative point of view, these quantities should be taken only as indicative considering the relative simplicity of the models used.

VI. CONCLUSION

It has been shown that NMR parameters like the ^{27}Al linewidth, spin-lattice relaxation rate and Knight shift are sensitive to structural changes as observed during recovery of LRO in disordered Ni_3Al. The linewidth, in particular, is affected by the existence of a distribution of Al sites resulting from the random distribution of the atoms on the lattice whereby the line broadening is enhanced by the presence of localized magnetic moments which may arise from the formation of small Ni clusters or dislocations during ball milling. The ^{27}Al NMR linewidth is proportional to the fraction of untransformed phase. Thus, systematic measurements as a function of annealing time and temperature give access to transformation kinetics and parameters like the activation energy of the ordering process. The activation energy of the ordering process is in good agreement with earlier published results deduced from other experimental methods.

A simple random-walk model of diffusion through vacancies can account for the functional dependence from time and temperature of the measured fraction of untransformed phase. In particular, the stretched-exponential form for the time dependence of the untransformed fraction finds a simple explanation in terms of the time dependence of the vacancy concentration during annealing. Based on the random-walk model, the number of elementary jumps that an atom does to reach its ordered position is found to be rather low.

Beyond the present work, two main features remain of great interest. The exact origin of the local Ni moment and its formation mechanism during ball milling should be further investigated experimentally as well as theoretically. Furthermore, the NMR technique seems very suitable to study the effects of the initial vacancy concentration on the kinetics of the ordering process.

ACKNOWLEDGMENTS

This work was supported in part by the Swiss National Foundation for Scientific Research. Ames Laboratory is operated for the U.S. Department of Energy by Iowa State University under Contract No. W-7405-ENG-82. The work at the Ames Laboratory was supported by the Office of Basic Energy Sciences. The authors are grateful to L. Jones, Ames Lab Material Preparation Center, for preparing the Ni_3Al samples and Ph. Bugnon, EPFL-IGA, for performing the XRD measurements.

*Present address: Laboratorio TASC-INFM, Padriciano 99, I-34012 Trieste.

[1] See various contributions, in *Ordering and Disordering in Alloys*, edited by A. R. Yavari (Elsevier, London, 1992).
[2] J. S. C. Jang and C. C. Koch, J. Mater. Res. **5**, 498 (1990).
[3] A. W. Weeker and H. Bakker, Physica B **153**, 93 (1988).
[4] C. L. Corey and D. I. Potter, J. Appl. Phys. **38**, 3894 (1967).
[5] T.-M. Wang, M. Shimotomai, and M. Doyama, J. Phys. F **14**, 37 (1984).
[6] M. D. Baro, J. Malagelada, S. Surinach, N. Clavaguera, and M. T. Clavaguera-Mora, in *Ordering and Disordering in Alloys* (Ref. 1), p. 55.
[7] R. Kozubski and M. C. Cadeville, J. Phys. F **18**, 2569 (1988).
[8] J. R. Caskey, J. M. Franz, and D. J. Sellmyer, J. Phys. Chem. Solids **34**, 1179 (1973).
[9] J. M. Koch and C. Koenig, Philos. Mag. B **55**, 359 (1987).
[10] G. C. Carter, L. H. Bennet, and D. J. Kahan, *Metallic Shifts in NMR* (Pergamon, New York, 1977).
[11] K. Aoki, X.-M. Wang, A. Memezawa, and T. Masumoto, Mater. Sci. Eng. A **179/180**, 390 (1994).
[12] F. Cardellini, F. Cleri, G. Mazzone, A. Montone, and V. Rosato, J. Mater. Res. **8**, 2504 (1993).
[13] A. R. Yavari, P. Crespo, E. Pulido, A. Hernando, G. Fillion, P. Lethuillier, M. D. Baro, and S. Surinach, in *Ordering and Disordering in Alloys* (Ref. 1), p. 12.
[14] T. J. Rowland, Prog. Mater. Sci. **9**, 1 (1961).
[15] R. A. Forman and A. H. Kahn, J. Chem. Phys. **45**, 4586 (1966).
[16] J. H. Van Vleck, Phys. Rev. **74**, 1168 (1948).
[17] A. Abragam, *The Principles of Nuclear Magnetism* (Oxford University Press, London, 1961).
[18] S. Rubini, C. Dimitropoulos, S. Aldrovandi, F. Borsa, D. R. Torgeson, and J. Ziolo, Phys. Rev. B **46**, 10 563 (1992).
[19] J. M. Brettell and W. S. Hinshaw, J. Phys. F **6**, 1177 (1976).
[20] D. Schumacher, W. Schüle, and A. Seeger, Z. Naturforsch. A **17A**, 228 (1962).
[21] H. R. Schober, W. Petry, and J. Trampenau, J. Phys.: Condens. Matter **4**, 9321 (1992).
[22] R. Gomer, Rep. Prog. Phys. **53**, 917 (1990).
[23] S. Chandrasekhar, Rev. Mod. Phys. **15**, 1 (1943).
[24] D. Althoff, D. Morgan, D. de Fontaine, M. Asta, S. M. Foiles, and D. D. Johnson, Phys. Rev. B **56**, 5705 (1997).